Catalysis Communications 11 (2010) 858–861

Contents lists available at ScienceDirect

Catalysis Communications

journal homepage: www.elsevier.com/locate/catcom

Effect of Ca doping on the catalytic performance of CuO–CeO_2 catalysts for methane combustion

Dongsheng Qiao [a], Guanzhong Lu [a,b,*], Dongsen Mao [b], Xiaohui Liu [a], Hongfeng Li [a], Yun Guo [a], Yanglong Guo [a]

[a] Key Laboratory for Advanced Materials and Research Institute of Industrial Catalysis, East China University of Science and Technology, Shanghai 200237, China
[b] Research Institute of Applied Catalysis, Shanghai Institute of Technology, Shanghai 200235, China

ARTICLE INFO

Article history:
Received 24 January 2010
Received in revised form 9 March 2010
Accepted 13 March 2010
Available online 19 March 2010

Keywords:
Methane
Catalytic combustion
CuO–CeO_2
Ca doping

ABSTRACT

Methane catalytic combustion was carried out over a series of Ca doped $Ce_{0.9-x}Cu_{0.1}Ca_xO_\delta$ ($0<x\leq0.3$) catalysts prepared by the citric acid complexation–combustion method. The catalyst with $x=0.05$ showed the optimum activity, with $T_{50}=478$ °C, 60 °C lower than that of Ca undoped catalyst. The Ca doping promoted the formation of oxygen vacancies of the catalyst. With the increase in Ca amount, more carbonate species were formed on the catalyst surfaces. The carbonate species produced on the catalysts after long-term reaction, were proposed to be responsible for the activity loss of the catalysts.

1. Introduction

The catalytic combustion of CH_4 has drawn considerable attention in the last decades due to its attractive industrial application in power and heat generation with ultralow emissions of NO_x, CO, and unburned hydrocarbons [1]. Moreover, the catalytic combustion is used to purify the exhausts of compressed natural gas (CNG) fueled vehicles [2], because methane is a well-known greenhouse gas. Generally, the catalysts containing noble metals such as Pd and Pt are active for methane combustion at low temperature [3], but they are expensive and poorly stable because of sintering and volatilization of the active phase at moderate–high temperatures [4,5]. Therefore, there is a strong demand to develop a new, thermally stable and low cost catalyst for the combustion of methane [6,7].

Recent reports showed that the copper-containing ceria catalysts exhibited good catalytic activity for the CH_4 combustion [8,9]. The high activity of CuO–CeO_2 composite is ascribed to strong interaction between the copper oxide and oxygen vacancies on ceria support at the interface boundary. In addition, the increase of oxygen bulk mobility of ceria-based catalysts, by introducing defective sites, seems to be effective for the promotion of hydrocarbon oxidation reactions [10,11]. It was reported that calcium doped CeO_2 would tend to introduce defects and oxygen vacancies in the CeO_2 fluorite structure, and also could lower the energy for charge transfer from oxygen ions to cerium ions [12,13].

However, to the best of our knowledge, there is no research work on exploring the effect of Ca doping on the CuO–CeO_2 composite oxide catalysts for the methane combustion. In the present work, a series of $Ce_{0.9-x}Cu_{0.1}Ca_xO_\delta$ ($x=0$, 0.01, 0.02, 0.05, 0.1, 0.15, and 0.3) composite oxides were prepared using citric acid complexation–combustion method, and their properties were characterized by the nitrogen adsorption/desorption, XRD, Raman, TG and FT-IR techniques. The influence of Ca doping on the properties of CuO–CeO_2 composite oxides for methane catalytic combustion is investigated.

2. Experimental

2.1. Catalyst preparation

The $Ce_{0.9-x}Cu_{0.1}Ca_xO_\delta$ ($x=0$–0.3) materials were prepared by the citric acid complexation–combustion method [14]. $Ce(NO_3)_3\cdot6H_2O$, $Cu(NO_3)_2\cdot3H_2O$ and $Ca(NO_3)_2\cdot2H_2O$ salts were dissolved in de-ionized water with suitable ratios. Citric acid was added with 1.2 times of molar amounts to the premixed nitrate solutions of cerium, copper and calcium. The obtained solution was stirred at 70 °C until the color of mixture solution changed from blue to green. Once the gel formed, the temperature was elevated to 150 °C quickly, and the gel foamed with production of nitrogen oxide vapors and burnt with sparks. A solid product was obtained after the sparks were extinguished. The as-obtained powder was calcined at 600 °C for 4 h in air and then grinded into 40–60 mesh, which is referred to fresh sample.

2.2. Catalyst characterization

Power X-ray diffraction patterns were recorded on Rigaku D/max 2250VB/PC diffractometer with Cu Kα radiation (λ = 1.5406) at scanning rate of 6°/min. The tube voltage and current were set at

* Corresponding author. Fax: +86 21 64253703.
E-mail address: gzhlu@ecust.edu.cn (G.Z. Lu).

1566-7367/$ – see front matter © 2010 Elsevier B.V. All rights reserved.
doi:10.1016/j.catcom.2010.03.010

40 KV and 100 mA, respectively. N_2 adsorption–desorption isotherms were measured at 77 K on a NOVA 4200e surface area and pore size analyzer. The samples were outgassed at 180 °C for 4 h before the measurement. The Brumauer–Emmett–Teller (BET) method was utilized to calculate the specific surface areas. The Raman spectra were obtained on a Renishaw Raman spectrometer equipped with a CCD detector at ambient temperature and moisture-free conditions. The emission line at 514.5 nm from an Ar^+ ion laser (Spectra Physics) was focused, analyzing spot about 1 mm, on the sample under the microscope. The infrared (IR) absorption spectra were recorded on a Nicolet NEXUS 670 FT-IR spectrometer, with 32 scans at an effective resolution of 4 cm^{-1}. The sample to be measured was ground with KBr and pressed into thin wafer for analysis.

2.3. Testing of catalytic activity

The catalytic activities of $Ce_{0.9-x}Cu_{0.1}Ca_xO_\delta$ catalysts for the methane combustion were carried out in a quartz tube reactor at atmospheric pressure. The reagent gas mixture consisted of 1.0% CH_4 + 4.0% O_2 in Ar at a total flow rate of 50 mL/min was passed through catalyst (0.10 g) bed, and the weight hourly space velocity (WHSV) was 30,000 mL/g h. The reactants and products were analyzed online by gas chromatograph (GC) equipped with TCD. The catalyst activity was characterized by T_{10}, T_{50} and T_{90} representing the temperatures at methane conversion of 10%, 50% and 90%, respectively.

3. Results and discussion

3.1. Catalyst characterization

3.1.1. X-ray diffraction

Fig. 1 shows the XRD patterns of CeO_2 and $Ce_{0.9-x}Cu_{0.1}Ca_xO_\delta$ samples with different Ca contents. The distinct diffraction pattern of CeO_2 is seen in all the samples. With the addition of Ca in the samples, no features of Ca species are visible in the patterns. It was reported that the maximum solubility limit of Ca^{2+} into CeO_2 is about 20 mol% [15], and $Ce_{1-x}Cu_xO_y$ ($x \leq 0.1$) solid solutions are obtained with low molar ratio of Cu/Ce [14]. Therefore, it could be suggested that Cu^{2+} and Ca^{2+} ions could simultaneously replace Ce^{4+} in the CeO_2 fluorite structure to form a solid solution $Ce_{0.9-x-y}Cu_{0.1-y}Ca_xO_\delta$ in the low doping amount of Cu^{2+} and Ca^{2+} ions. Moreover, with the increase in the Ca^{2+} amount in the samples, the lattice constants of ceria increase from 0.5392 nm to 0.5416 nm (Table 1) and the XRD reflections of the cubic ceria slightly shift to lower degrees, which confirm further that the solid solution is formed after larger size of Ca^{2+} (1.12 Å) substitutes for Ce^{4+} (0.97 Å) inside the c-CeO_2 structure [16]. The results in Table 1 also show that, the Ca doping in the samples led to a decrease in the BET surface areas from 38.9 m^2/g to 19.8 m^2/g, and also to a decrease in the CeO_2 crystallite size from 10.2 nm to 7.8 nm. J. Papavasiliou et al. [17] also reported that addition of dopant (La, Mg, Y or Ca) in CuO–CeO_2 could cause a decrease in the surface area, which was not accompanied with a prospective increase in the CeO_2 crystallite size.

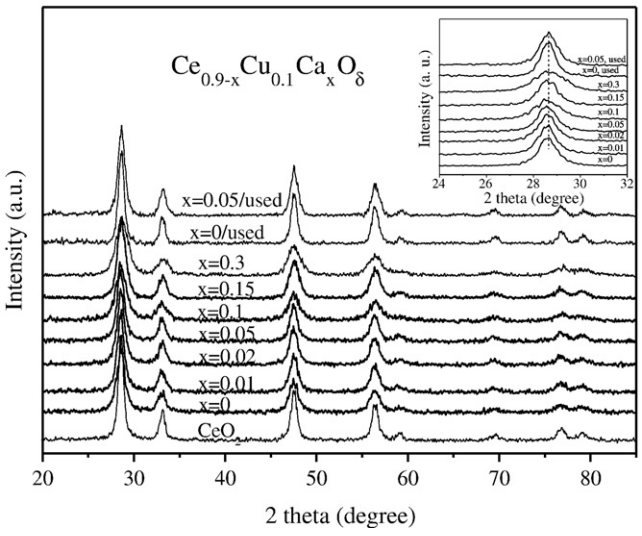

Fig. 1. XRD patterns of CeO_2 and $Ce_{0.9-x}Cu_{0.1}Ca_xO_\delta$ catalysts.

3.1.2. IR absorption spectroscopy

IR spectra of the prepared $Ce_{0.9-x}Cu_{0.1}Ca_xO_\delta$ samples are presented in Fig. 2. The bands at about 1065, 1350 and 1520 cm^{-1} were detected on the sample with $x = 0$, which should be corresponded to carbonate species [18]. It was reported by S. Hilaire et al. [19] that the formation of carbonates is favored in solids containing CeO_2. P. Djinović et al. [20] also reported that carbonate-like species are present on the surface of CuO–CeO_2 mixed oxides, due to the basicity of the sample. So, it is deduced that carbonate species probably in the form of Cu or Cerium carbonates might be formed, due to the adsorption of surrounding gas molecule. The bands at 879 and 1450 cm^{-1} should be assigned to carbonate calcium phase [21,22], and the intensity of these bands is enhanced obviously with an increase in x values. Therefore, it indicates that surface carbonates are present in the samples for lower Ca content, and more carbonate species mainly in the form of isolated bulk carbonate calcium are present in the samples for higher Ca content.

3.1.3. Raman spectroscopy

Fig. 3 shows the Raman spectra of $Ce_{0.9-x}Cu_{0.1}Ca_xO_\delta$ samples. A broad band with relatively high intensity at about 460 cm^{-1} and a weak band at 1185 cm^{-1} were observed, which are ascribed to the F_{2g} vibration mode and primary A_{1g} asymmetry of pure CeO_2 respectively [23]. The band around 605 cm^{-1} can be linked to lattice defects that result from the produced oxygen vacancies in the ceria fluorite structure [24]. With the increase in Ca addition, the intensity of the band at 605 cm^{-1} increases accordingly and reaches maximum at $x = 0.05$. Moreover, the band 460 cm^{-1}ascribed to the F_{2g} mode of CeO_2 shifts slightly to lower wave number region as shown in the enlarged graphic in Fig. 3, which should be due to the solid solution formation and the changes in the lattice parameter with particle size [25]. When $x > 0.1$ in the samples, the band at 605 cm^{-1} in their Raman spectra decreases gradually, suggesting that the samples might be covered by the increasing amount of the carbonate species as shown in Fig. 2.

3.2. Performance of catalyst for methane combustion

Catalytic activities of $Ce_{0.9-x}Cu_{0.1}Ca_xO_\delta$ for methane combustion are listed in Table 1, and are expressed with the values of T_{10}, T_{50} and T_{90}, which are the temperatures at methane conversion of 10%, 50%

Table 1
The BET surface areas (SA), lattice constants (a), crystallite sizes of cubic ceria phase d (1 1 1) and the temperatures of 10%, 50% and 90% of CH_4 conversion over fresh and used samples.

Catalyst	T_{10} (°C)	T_{50} (°C)	T_{90}(°C)	a (nm)	d (nm)	SA (m^2/g)
$Ce_{0.9}Cu_{0.1}O_\delta$	427	538	629	0.5392	10.2	38.9
$Ce_{0.89}Cu_{0.1}Ca_{0.01}O_\delta$	420	509	603	0.5394	10.6	32.3
$Ce_{0.87}Cu_{0.1}Ca_{0.02}O_\delta$	408	501	596	0.5400	9.6	31.7
$Ce_{0.85}Cu_{0.1}Ca_{0.05}O_\delta$	388	478	555	0.5403	9.5	31.3
$Ce_{0.8}Cu_{0.1}Ca_{0.1}O_\delta$	422	515	610	0.5406	8.7	26.6
$Ce_{0.75}Cu_{0.1}Ca_{0.15}O_\delta$	430	564	662	0.5411	8.4	22.0
$Ce_{0.6}Cu_{0.1}Ca_{0.3}O_\delta$	486	612	694	0.5416	7.8	19.8
$Ce_{0.9}Cu_{0.1}O_\delta$-used	–	–	–	0.5391	12.0	31.1
$Ce_{0.85}Cu_{0.1}Ca_{0.05}O_\delta$-used	–	–	–	0.5396	10.5	29.5

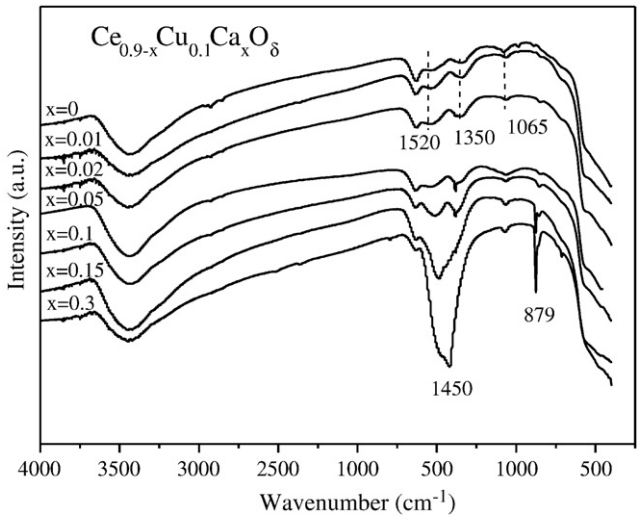

Fig. 2. IR spectra of $Ce_{0.9-x}Cu_{0.1}Ca_xO_\delta$ catalysts.

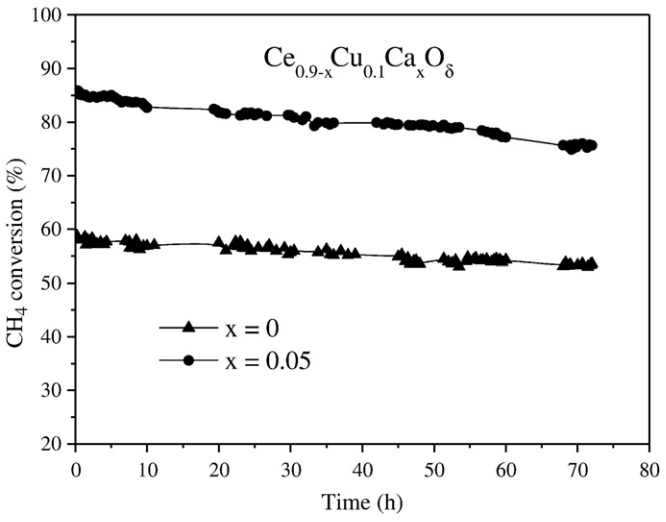

Fig. 4. Evolution of methane conversion at 550 °C over $Ce_{0.9-x}Cu_{0.1}Ca_xO_\delta$ catalysts.

and 90%, respectively. During methane combustion reaction, CH_4 was completely oxidized to CO_2 and H_2O. When $x<0.15$ in the samples, the activities of catalysts are apparently superior to that of Ca undoped catalyst, and the catalyst with $x=0.05$ presents the best activity, with $T_{10}=388$ °C, $T_{50}=478$ °C and $T_{90}=550$ °C. It is well-known that an increase in oxygen bulk mobility of ceria-based catalysts, by introducing defective sites, is effective to promote the hydrocarbon oxidation reactions [26]. Therefore, the high activity of catalyst with $x=0.05$ should be attributed to the much more oxygen vacancies formed by doping Ca in the CeO_2 fluorite structure, which is in good agreement with the Raman results (Fig. 3). When the Ca amount increase further ($x\geq 0.1$), the activity of catalyst declined gradually, which should be owed to the carbonate species formed on the catalyst surface (seen IR spectra in Fig. 2), resulting in the coverage of the active sites. Based on the above results, it is concluded that, doping proper amount of Ca in the $Ce_{0.9-x}Cu_{0.1}Ca_xO_\delta$ catalysts can improve the activities of the catalysts by promoting the formation of the oxygen defective sites.

In order to test the long-term activity of the $Ce_{0.9-x}Cu_{0.1}Ca_xO_\delta$ catalyst, its life-time was tested over fresh samples with $x=0$ and 0.05. The catalytic reaction occurred at 550 °C for 72 h, and WHSV was 30,000 mL/g h. As shown in Fig. 4, a slight loss of activity with the reaction time was observed for these two catalysts. Over the sample without Ca, the methane conversion is 59% for 1 h, and decreases to 53% for 72 h; over the doped-Ca catalyst, the methane conversion is 85% for 1 h and 76% for 72 h. It shows that the presence of Ca in the catalyst can remarkably improve its catalytic performance for methane combustion in the long-term reaction.

To explain the deactivation of the catalysts in the methane oxidation, the FT-IR spectra and XRD characterization of the used catalysts were carried out and the results are exhibited in Fig. 1 and Fig. 5. The results show that, more intensive bands at 1080, 1350 and 1520 cm^{-1} are observed, as compared with the fresh ones. It is demonstrated that much more carbonate species are formed on the used samples, which could block the active sites to result in the deactivation of the catalysts. Based on the XRD results, it is obtained that for the used Ca doped sample the lattice constant of ceria is smaller than that in the fresh one (Table 1), which indicates that during operation Ca went out from the bulk to the surface forming CeO_2 with lower Ca content and additional carbonates, which would lead to the decrease of sample activity during operation. Moreover, an increase in crystal size and a decrease in BET surface areas of the used samples are shown in Table 1, which would also contribute to the activity loss of the catalysts.

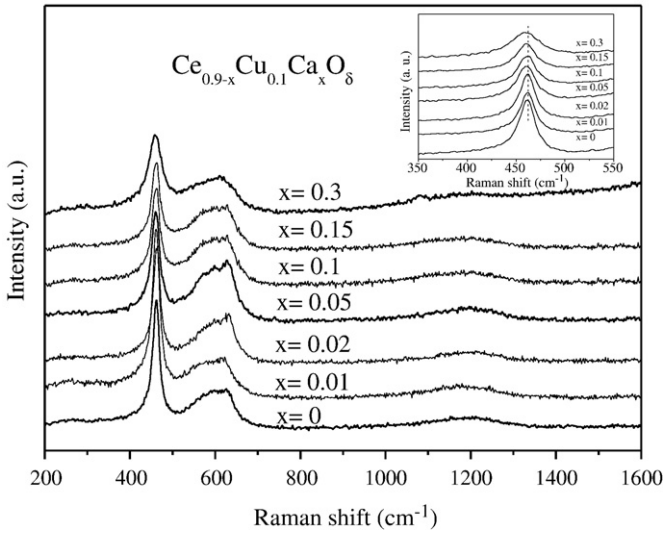

Fig. 3. Raman spectra of $Ce_{0.9-x}Cu_{0.1}Ca_xO_\delta$ catalysts.

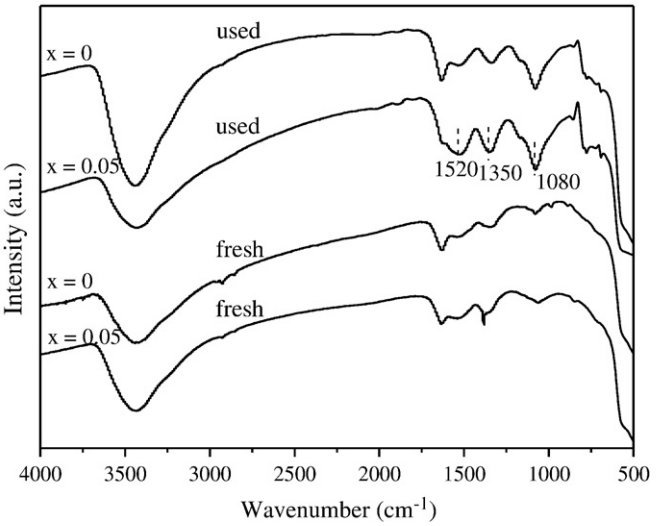

Fig. 5. IR spectra of used $Ce_{0.9-x}Cu_{0.1}Ca_xO_\delta$ catalysts.

4. Conclusions

In summary, it has been found that the $Ce_{0.9-x}Cu_{0.1}Ca_xO_\delta$ solid solution is formed with Ca and Cu ions simultaneously distributed in the CeO_2 fluorite structure. The catalyst with $x = 0.05$, behaves the best catalytic performance for methane combustion, that is, $T_{10} = 388$ °C and $T_{90} = 550$ °C. The presence of Ca in the catalyst favors the formation of oxygen vacancies, resulting in a remarkable enhancement of the catalytic performance for methane combustion. More carbonate species mainly in the form of calcium carbonate are formed with higher Ca content in the sample. After the catalyst is used in the methane combustion for a long time, the Ca could migrate to the surface of the Ca doped catalyst and the carbonate species were formed on the surface of used catalysts, which should be responsible for the activity loss of catalysts.

Acknowledgements

We would like to acknowledge the financial support from the National Basic Research Program of China (no. 2010CB732300) and the Education Committee of Shanghai (no. J51503).

References

[1] P. Forzatti, G. Groppi, Catal. Today 54 (1999) 165–180.
[2] J.K. Lampert, M.S. Kazi, R.J. Farrauto, Appl. Catal. B: Environ. 14 (1997) 211–223.
[3] T.V. Choudhary, S. Banerjee, V.R. Choudhary, Appl. Catal. A: Gen. 234 (2002) 1–23.
[4] K. Persson, A. Ersson, K. Jansson, N. Iverlund, S.G. Jaras, J. Catal. 231 (2005) 139–150.
[5] K. Persson, K. Jansson, S.G. Jaras, J. Catal. 245 (2007) 401–414.
[6] V.C. Belessi, A.K. Ladavos, P.J. Pomonis, Appl. Catal. B: Environ. 31 (2001) 183–194.
[7] J. Cheng, H.L. Wang, Z.P. Hao, S.B. Wang, Catal. Commun. 9 (2008) 690–695.
[8] W. Liu, M.F. Stephanopoulos, J. Catal. 153 (1995) 304–316.
[9] P. Bera, K.C. Patil, V. Jayaram, G.N. Subbanna, M.S. Hegde, J. Catal. 196 (2000) 293–301.
[10] D. Terribile, A. Trovarelli, C. Leitenburg, A. Primavera, G. Dolcetti, Catal. Today 47 (1999) 133–140.
[11] L.F. Liotta, G.D. Carlo, G. Pantaleo, G. Deganello, Catal. Commun. 6 (2005) 329–336.
[12] S. Carolis, J.L. Pascual, L.G.M. Pettersson, J. Phys. Chem. B 103 (1999) 7627–7636.
[13] J.A. Rodriguez, X.Q. Wang, J.C. Hanson, G. Liu, J. Chem. Phys. 119 (2003) 5659–5669.
[14] W.J. Shan, W.J. Shen, C. Li, Chem. Mater. 15 (2003) 4761–4767.
[15] M. Yan, T. Mori, F. Ye, D.R. Ou, J. Zou, J. Drenna, J. Eur. Ceram. Soc. 28 (2008) 2709–2716.
[16] M. Yamashita, K. Kameyama, S. Yabe, S. Yoshida, Y. Fujishiro, T. Kawai, T. Sato, J. Mater. Sci. 37 (2002) 683–687.
[17] J. Papavasiliou, G. Avgouropoulos, T. Ioannides, Appl. Catal. B: Environ. 69 (2007) 226–234.
[18] O. Pozdnyakova, D. Teschner, A. Woostsch, J. Krohnert, B. Steinhauer, H. Dauer, L. Toh, F.C. Jentoft, A. Knop-Gericke, Z. Paal, R. Schlogl, J. Catal. 237 (2006) 1–16.
[19] S. Hilaire, X. Wang, T. Luo, R.J. Gorte, J. Wagner, Appl. Catal. A 215 (2001) 271–278.
[20] P. Djinović, J. Levec, A. Pintar, Catal. Today 138 (2008) 222–227.
[21] A. Mikkelsen, S.B. Engelsen, H.C.B. Hansen, O. Larsen, L.H. Skibsted, J. Cryst. Growth 177 (1997) 125–134.
[22] G. Pecchi, P. Reyes, R. Zamora, C. Campos, L.E. Cadús, B.P. Barbero, Catal. Today 133 (2008) 420–427.
[23] W.H. Weber, K.C. Hass, J.R. McBride, Phys. Rev. B 48 (1993) 178–185.
[24] J.R. McBride, K.C. Hass, B.D. Poindexter, W.H. Weber, J. Appl. Phys. 76 (1994) 2435–2441.
[25] J.E. Spanier, R.D. Robinson, F. Zhang, S.W. Chan, I.P. Herman, Phys. Rev. B 64 (2001) 245407–245414.
[26] D. Wolf, Catal. Lett. 27 (1994) 207–220.